The effect of non-uniform microscale distribution of sorption sites on solute diffusion in soil

S . A . M a s u m[a,b], G . J . D . K i r k[b], K . R . D a l y[a] & T . R o o s e[a]

[a]*Bioengineering Sciences Research Group, Engineering Sciences, Faculty of Engineering and Environment, University of Southampton, Southampton, SO17 1BJ, UK, and* [b]*School of Water, Energy and Environment, Cranfield University, Cranfield, MK43 0AL, UK*

Summary

Conventional models of solute transport in soil consider only soil volumes large enough to average over microscale heterogeneities, and it is assumed that microscale variations are unimportant at the macroscale. In this research we test this assumption for cases in which the microscale distribution of solute-sorbing sites is patchy. We obtain a set of equations at the macroscale that allow for the effect of the microscale distribution with the mathematical technique of homogenization. We combine these equations with an image-based model that describes the true microscale pore geometry in a real, structured soil measured with X-ray computed tomography. The resulting models are used to test the microscale averaging assumptions inherent in conventional models. We show that, in general, macroscale diffusion is little affected by microscale variation in the distribution of sorption sites. Therefore, for most purposes the assumption of microscale averaging used in conventional models is justified. The effects of microscale heterogeneity are noticeable only when (i) the rate of sorption is slow compared with diffusion, but still fast enough to affect macroscale transport and (ii) the defined macroscale volume approaches the microscale. We discuss the effects when these conditions are met.

Highlights

- When does microscale variation need to be allowed for in macroscale transport and reaction models?
- We use image-based modelling and homogenization to answer this.
- We find macroscale transport is generally little affected by microscale patchiness of sorption sites.
- The microscale averaging implicit in conventional models is justified in most cases.

Introduction

Soil is heterogeneous at all scales, but the degree of heterogeneity increases the finer the scale considered. For instance, at the scale of a root hair or fungal hypha, the distribution of mineral and organic matter surfaces on which nutrient and pollutant solutes are sorbed is patchy, and the patches have varying sizes and distributions. With advances in non-invasive imaging techniques, it is increasingly possible to quantify such heterogeneities and, in principle, to allow for them in models of soil processes (Leitner *et al.*, 2010; Blunt *et al.*, 2013; Keyes *et al.*, 2013; Wildenschild & Sheppard, 2013). The research in this paper assesses the circumstances in which it is worth doing this.

Conventional models of solute transport and reaction in soil treat the soil as quasi-homogeneous by considering only soil volumes large enough to average over microscale variation (Tinker & Nye, 2000). The questions are: what are the limiting volumes for which this is justified and how do they depend on microscale heterogeneities and reaction rates relative to transport rates? We aim to answer these questions below.

We use the mathematical method of homogenization (Hornung, 1997; Pavliotis & Stuart, 2008) to derive macroscale equations for solute transport and reaction that allow for microscale heterogeneities. This method has been used widely to derive soil hydraulic properties (Keller, 1980; Daly *et al.*, 2015; Tracy *et al.*, 2015), poroelastic properties (Burridge & Keller, 1981; Lee & Mei, 1997) and solute effective diffusivities (Ptashnyk *et al.*, 2010; Zygalakis *et al.*, 2011). We use homogenization in conjunction

with image-based modelling (Keyes *et al.*, 2013; Daly *et al.*, 2015; Tracy *et al.*, 2015). Image-based modelling is the use of two- or three-dimensional images to derive true geometries on which to base mathematical models. Here we use three-dimensional images, generated with X-ray computed tomography (X-ray CT), to derive the true geometric impedance to solute transport in a particular experimental soil.

By combining image-based modelling with equations for time-dependent sorption reactions on the soil surfaces, we can allow for patchy distributions of the sorption sites. The resulting models enable us to test the assumption of microscale averaging used in conventional models.

Theory

The nomenclature is explained in Table 1. Table S1 in Supplementary Information provides further explanation about the mathematical symbols.

Dimensional model

We consider the transport of a solute through a soil volume across which there is a concentration gradient of the solute. The solute is distributed between the soil solution, where it is mobile, and the surfaces of soil particles, where it is sorbed and immobile. Unlike conventional models, the spatial distribution of sorption sites is considered to be patchy (i.e. there are areas of the soil surface where sorption does occur and areas where it does not). The sorption reactions we consider are either fast or slow in comparison with transport through the soil solution. For simplicity we consider a soil in which the pores are completely filled with solution and transport is solely by diffusion. Note, however, that it would be straightforward to model partially saturated soil by including air spaces in the pores.

To model the effects of a patchy distribution of sorption sites, we use the method of homogenization. The key requirement of this method is that the macroscale (observable) properties are, on average, independent of the microscale properties. Therefore, at the macroscale we do not need to know the exact paths taken by the solute. Rather, we need consider only the average solute flux through a microscale volume of soil. We use the microscale geometrical details to parameterize a set of macroscale equations that allow for the microscale detail through a representative 'cell problem' (Hornung, 1997; Pavliotis & Stuart, 2008). If we consider that the macro- and microscale spatial properties are independent of each other, we can define the macro- and microscale coordinate systems as **x** and **y**, respectively. This is illustrated in Figure 1. The characteristic macroscopic length-scale, *L*, is the length of the macroscopic unit in Figure 1(a) and the microscopic length-scale, *l*, is the length of the microscopic unit cell in Figure 1(b). Formally, homogenization theory allows us to treat **x** and **y** independently if the scaling ratio $\varepsilon = l/L$ is sufficiently small (i.e. $\varepsilon \ll 1$) (Pavliotis & Stuart, 2008).

We now consider the behaviour of the microscale domain in detail. Our aim is to derive a set of equations that can be applied

Table 1 Nomenclature

Symbol	Definition	Units
A_f, A_s	Surface area per unit soil volume of fast, slow sorption sites	$cm^2\,cm^{-3}$
C_{af}, C_{as}	Solute concentration on fast, slow sorption surfaces	$\mu mol\,cm^{-2}$
C_l	Solute concentration in soil solution	$\mu mol\,cm^{-3}$
D_l	Solute diffusion coefficient in free solution	$cm^2\,s^{-1}$
k_{af}, k_{as}	Rate constant for fast, slow adsorption	$cm\,s^{-1}$
k_{df}, k_{ds}	Rate constant for fast, slow desorption	s^{-1}
K_f, K_s	Equilibrium solid: solution distribution for fast, slow sorption sites	–
l	Characteristic microscopic length scale	cm
L	Characteristic macroscopic length scale	cm
$\mathbf{x}$	Macroscopic space variable	cm
$\mathbf{y}$	Microscopic space variable	cm
α	Ratio of slow to fast sorption surface areas	–
ε	Scaling ratio $= l/L$	–
δ_{af}, δ_{as}	Dimensionless parameter for fast, slow adsorption	–
δ_{df}, δ_{ds}	Dimensionless parameter for fast, slow desorption	–
$\mathbf{D}$	Tensor for the geometric tortuosity of the solution diffusion path (dimensionless)	–
$\mathbf{E}$	Tensor to represent the effect of random phase distribution for fast sorption reaction (dimensionless)	–
$\mathbf{f}$	Vector to represent the effect of random phase distribution for slow sorption reaction (dimensionless)	–
Γ	Domain of total soil particle surface	–
Γ_s	Domain of sorption sites on soil surfaces	–
Γ_{ns}	Domain of non-sorbing sites on soil surfaces	–
Ω	Domain of soil solution	–
∇	Partial differential operator in 3D space $(= \partial/\partial x, \partial/\partial y, \partial/\partial z)$	cm^{-1}

to the macroscale and a set of cell problems that capture the geometrical effects of the microscale domain. We define the soil solution domain as Ω and the total soil surface domain as Γ; Γ is subdivided into a domain of solute-sorbing sites, Γ_s, and a domain of non-sorbing sites, Γ_{ns}. Then, the diffusive transport of a solute in the soil solution is given by:

$$\frac{\partial C_l}{\partial t} = D_l \nabla^2 C_l, \quad \mathbf{x} \in \Omega, \tag{1}$$

where C_l is the concentration of the solute in the soil solution and D_l is its diffusion coefficient in free solution.

We define the amount of solute sorbed per unit of soil surface area in fast and slow reactions as C_{af} and C_{as}, respectively. The boundary conditions at the interface between soil surfaces and the solution for
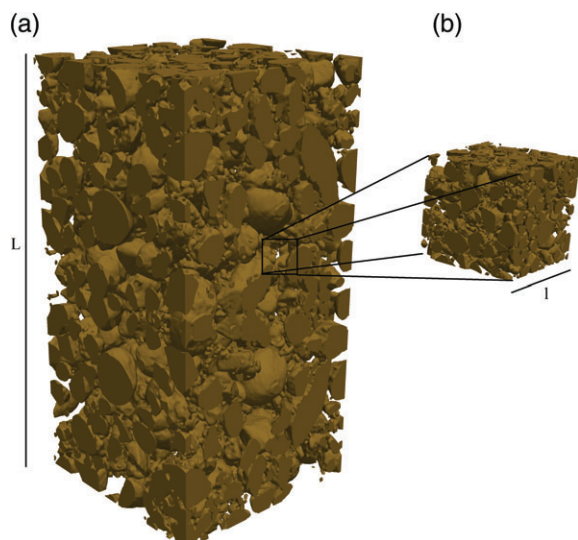
Figure 1 The geometry of the model: (a) the macroscopic domain with characteristic length-scale L; (b) the microscopic domain with length-scale l. The microscopic domain contains non-uniformly distributed soil solution and soil surfaces with solute-sorption sites. The microscopic heterogeneity is repeated and periodic in the macroscopic domain. The figure is taken from an X-ray CT image of a sandy loam.

sorbing surfaces are:

$$\mathbf{n} \cdot D_1 \boldsymbol{\nabla} C_1 = -\frac{\partial C_{af}}{\partial t} - \frac{\partial C_{as}}{\partial t} \quad \mathbf{x} \in \Gamma_s, \tag{2}$$

and for non-sorbing soil surfaces

$$\mathbf{n} \cdot D_1 \boldsymbol{\nabla} C_1 = 0, \quad \mathbf{x} \in \Gamma_{ns}, \tag{3}$$

where $\mathbf{n}$ is a unit vector that is normal to the soil surface and points into the soil solution. Mass conservation is accommodated with linear first-order sorption reactions as follows:

$$\frac{\partial C_{af}}{\partial t} = k_{af} C_1 - k_{df} C_{af}, \quad \mathbf{x} \in \Gamma_s, \tag{4}$$

$$\frac{\partial C_{as}}{\partial t} = k_{as} C_1 - k_{ds} C_{as}, \quad \mathbf{x} \in \Gamma_s, \tag{5}$$

where k_{af}, k_{df}, k_{as} and k_{ds} are the spatially-dependent rate constants for fast and slow adsorption and desorption reactions, respectively.

Non-dimensionalization

To proceed with the analysis, we express Equations (1)–(5) in non-dimensional forms so that there are fewer parameters to deal with and it is easier to determine which processes are most important for any given parameter regime. We do this by scaling space with the macroscale length, $\mathbf{x} = L\mathbf{x}^*$, and time with the macroscale diffusion time, $t = \frac{L^2}{D_1} t^*$, where the asterisks indicate dimensionless variables. We scale the solution concentrations with unit

concentration as $C_1 = [C]C_1^*$, where C is a representative solute concentration in solution. Likewise, the sorbed concentrations are scaled as $C_{af} = \left(\frac{k_{af}}{k_{df}}\right)[C]C_{af}^*$ and $C_{as} = \left(\frac{k_{as}}{k_{ds}}\right)[C]C_{as}^*$ to balance the adsorption and desorption terms in Equations (4) and (5).

Next, we non-dimensionalize the equations to reduce the number of parameters in the model, and then re-scale to estimate the importance of each of these parameters, as follows (without the asterisks):

$$\frac{\partial C_1}{\partial t} = \nabla^2 C_1, \quad \mathbf{x} \in \Omega, \tag{1a}$$

$$\mathbf{n} \cdot \boldsymbol{\nabla} C_1 = -\delta_{af}\left(C_1 - C_{af}\right) - \varepsilon \delta_{as}\left(C_1 - C_{as}\right), \quad \mathbf{x} \in \Gamma_s, \tag{2a}$$

$$\mathbf{n} \cdot \boldsymbol{\nabla} C_1 = 0, \quad \mathbf{x} \in \Gamma_{ns}, \tag{3a}$$

$$\frac{\partial C_{af}}{\partial t} = \varepsilon^{-1}\delta_{df}\left(C_1 - C_{af}\right), \quad \mathbf{x} \in \Gamma_s, \tag{4a}$$

$$\frac{\partial C_{as}}{\partial t} = \varepsilon \delta_{ds}\left(C_1 - C_{as}\right), \quad \mathbf{x} \in \Gamma_s, \tag{5a}$$

where $\delta_{af} = \left(\frac{L}{D_1}\right) k_{af}$, $\delta_{df} = \left(\frac{L \cdot l}{D_1}\right) k_{df}$, $\delta_{as} = \left(\frac{L^2}{l \cdot D_1}\right) k_{as}$ and $\delta_{ds} = \left(\frac{L \cdot l}{D_1}\right) k_{ds}$. We have scaled Equations (1a)–(5a) such that the parameters in the equations are all of size one. The only exception is the small parameter ε that we use in the forthcoming derivation. The parameters δ_{af}, δ_{df}, δ_{as} and δ_{ds} are all dimensionless because of the difference in dimensions in the adsorption and desorption constants; their values are given in Table S1 in the supporting information.

Homogenized models

We apply the method of homogenization to Equations (1a)–(5a) to obtain effective macroscale models. Homogenization is a multi-scale method based on a standard perturbation expansion in which both the dependent and independent variables (in this case the concentrations and the spatial coordinates) are expanded. This is essentially an averaging procedure that allows the effect of the micro-structure to be determined as a series of effective parameters. A full description of the method and mathematical details are included in the Supporting Information S1. In short, we consider the behaviour of Equations (1a)–(5a) on two scales, the micro- then the macroscale, and consider gradients on the macroscale as a perturbation to the microscale equations. There are three key steps. First, we show that, as a first approximation, the nutrient concentrations are independent of the microscale geometry. Physically, this means that diffusion at the microscale is so fast that the concentration is effectively constant. Second, we consider that although the concentration may be considered constant at the microscale, it may vary at the macroscale. If the concentration changes linearly by one unit over unit distance, it must also change by a quantity of size ε over a distance ε. Therefore, we treat any variation in the macroscale concentration as a perturbation on the microscale. In addition, we have

perturbations that arise from reactions at the soil particle surfaces. The result is that we must solve a set of representative problems at the microscale that we refer to as cell problems. Typically, these problems describe how the microscale geometry affects diffusion at the macroscale and they must be solved numerically for all but the simplest geometries. Finally, by averaging over the microscale we can eliminate all effects of the microstructure from the problem and are left with a series of macroscale equations. These are parameterized by a set of effective parameters, which are calculated by solving the cell problems on the underlying microstructure.

We present two examples; each requires a separate homogenized model. In Case 1, the fast sorption reaction is effectively instantaneous and the slow reaction is slow in comparison with diffusion through the soil solution (discussed further in *Parameter values*). In Case 2, the slow reaction is 100-fold slower (i.e. k_{as} is 100-fold smaller than in Case 1). We summarize the models for the two examples in this section and provide full details in the Supporting Information, SI.

To derive the macroscale equations, we use the following asymptotic expansion of the concentration variables with respect to ε as follows:

$$C_1 = C_1^0(\mathbf{x}) + \varepsilon C_1^1(\mathbf{x}) + O\left(\varepsilon^2\right),$$
$$C_{af} = C_{af}^0(\mathbf{x}) + \varepsilon C_{af}^1(\mathbf{x}) + O\left(\varepsilon^2\right),$$
$$C_{as} = C_{as}^0(\mathbf{x}) + \varepsilon C_{as}^1(\mathbf{x}) + O\left(\varepsilon^2\right), \qquad (6)$$

where $C_1^0(\mathbf{x})$, $C_{af}^0(\mathbf{x})$ and $C_{as}^0(\mathbf{x})$ are the leading order macroscale solute concentrations in solution and on the fast and slow sorption sites, respectively, and $O(\varepsilon^2)$ indicates remainder terms. These leading order concentrations represent the effect of phase distribution for uniform distribution of sorbing phases. The concentrations for the non-uniform sorbing phase distributions on the soil surface are found as a perturbation to the average concentration and are given by $C_1^1(\mathbf{x})$, $C_{af}^1(\mathbf{x})$ and $C_{as}^1(\mathbf{x})$.

If Equation (6) is substituted into Equations (1a)–(5a) we obtain, after the mathematical derivation given in Supporting Information B in Appendix S1, a homogenized macroscale model for Case 1:

$$\tau \frac{\partial C_1^0}{\partial t} + \delta_{as} ||\Gamma_s|| C_1^0 = \mathbf{\nabla} \cdot \mathbf{D} \, \mathbf{\nabla} \, C_1^0, \qquad (7)$$

where $\mathbf{D}$ is a second-rank tensor that accounts for the geometric tortuosity of the solution diffusion pathway. Its value is obtained by solving the cell equations for the microscale pore space as shown in the supporting information. The reaction time constant (τ) in Equation (7) is:

$$\tau = ||\Omega|| + \frac{\delta_{af}}{\delta_{df}} ||\Gamma_s||, \qquad (8)$$

where $||\Gamma_s||$ and $||\Omega||$ are the magnitudes of the non-dimensional sorbing phase area and soil solution volume, respectively. By considering terms of higher powers in ε, the macroscale homogenized model that allows for non-uniform spatial distribution of sorption phases is:

$$\tau \frac{\partial C_1^1}{\partial t} + \delta_{as} ||\Gamma_s|| \left(C_1^1 - C_{as}^1 \right) = \mathbf{\nabla} \cdot \mathbf{D} \, \mathbf{\nabla} \, C_1^1$$
$$+ \mathbf{\nabla} \cdot \mathbf{E} \, \mathbf{\nabla} \, \mathbf{\nabla} \, C_1^0 + \mathbf{\nabla} \cdot \mathbf{f} C_1^0 + \frac{\delta_{af}}{\delta_{df}^2} ||\Gamma_s|| \frac{\partial^2 C_1^0}{\partial t^2}, \qquad (9)$$

where $\mathbf{E}$ is a third-rank tensor that accounts for the distribution of fast sorption sites and $\mathbf{f}$ is a vector that accounts for the distribution of slow sorption sites in the microscale domain (detail is provided in Supporting Information A and B). In addition:

$$\frac{\partial C_{as}^1}{\partial t} = \delta_{ds} C_1^0. \qquad (10)$$

We now present the effective macroscale models for Case 2 where the slow sorption reaction is 100 times slower than in Case 1. The effective macroscale model with uniform sorption-site distribution is the conventional model for macro-scale diffusive transport:

$$\tau \frac{\partial C_1^0}{\partial t} = \mathbf{\nabla} \cdot \mathbf{D} \, \mathbf{\nabla} \, C_1^0, \qquad (11)$$

and the homogenized model at order $O(\varepsilon)$ is

$$\tau \frac{\partial C_1^1}{\partial t} + \delta_{as} ||\Gamma_s|| C_1^0 = \mathbf{\nabla} \cdot \mathbf{D} \, \mathbf{\nabla} \, C_1^1 + \mathbf{\nabla} \cdot \mathbf{E} \, \mathbf{\nabla} \, \mathbf{\nabla} \, C_1^0 + \frac{\delta_{af}}{\delta_{df}^2} ||\Gamma_s|| \frac{\partial^2 C_1^0}{\partial t^2}. \qquad (12)$$

The diffusive behaviour of the solutes at the macroscale is the same as for Case 1. In this example however, the slow reaction is present, to leading order, only through the effective time constant τ, Equation (11). The effect of the slow reaction is described by Equation (12) and can be seen to contribute to C_1^1. In Case 1 the effect of the non-uniform sorption sites was described by the vector $\mathbf{f}$, see Equation (9). In this example these terms do not occur until the next order. In other words, as the reaction is slowed down it produces a weaker effect on the overall solute concentration.

In summary, the homogenized macroscale equations suggest that the maximal effect of the spatial distribution of sorption sites occurs with the parameter regime in Case 1. At this point it is natural to ask whether there is a reaction rate for which the non-uniformity of sorption sites has a larger effect on solute transport. If we slow the reactions down further, then this effect is simply pushed to the higher orders (i.e. it becomes smaller). Alternatively, if we increase the speed of the slow reaction then it becomes comparable to, or faster than, diffusion. If this is the case then we see only the averaged effects. In all cases, the effect of non-uniform distribution of sorption sites appears to be at least an order later than that of averaged or uniform distributions, which indicates that the non-uniform distribution has a small effect only on the macroscale diffusion. Physically, this indicates that as the size of the macroscale domain (i.e. *L*) increases, the effects of the non-uniform distribution decrease. We illustrate this point further below.

We rescale the dimensionless terms in the macroscale homogenized equations with the corresponding scales given in the

non-dimensionalization section above. The dimensional forms of Equations (7) and (9) are:

$$\frac{\partial \left(\theta + K_f \right) C_1^0}{\partial t} + (1/L)\, k_{as} C_1^0 = \nabla \cdot \mathbf{D}_{eff} \, \nabla\, C_1^0 \quad (13)$$

and

$$\frac{\partial \left(\theta + K_f \right) C_1^1}{\partial t} + (1/L)\left(k_{as} C_1^1 - k_{ds} C_{as}^1 \right) = \nabla \cdot \mathbf{D}_{eff} \, \nabla\, C_1^1$$

$$+ \nabla \cdot \mathbf{E}_{eff} \, \nabla \, \nabla\, C_1^0 + \nabla \cdot \mathbf{f}_{eff} C_1^0 + \frac{L k_{af}}{D_l k_{df}} \frac{\partial^2 C_1^0}{\partial t^2}, \quad (14)$$

where $\mathbf{D}_{eff} = D_l \mathbf{D}$, $\mathbf{E}_{eff} = L D_l \mathbf{E}$ and $\mathbf{f}_{eff} = \mathbf{f} D_l / L$ are the effective homogenized model parameters with units $cm^2\, s^{-1}$, $cm^3\, s^{-1}$ and $cm\, s^{-1}$, respectively, θ is the soil volumetric water content, and K_f and K_s are the equilibrium distributions of solute between the surface sites and the soil solution, given by:

$$K_f = \frac{A_f C_{af}}{\theta C_1}. \quad (15)$$

and

$$K_s = \frac{A_s C_{as}}{\theta C_1}. \quad (16)$$

The dimensional form of Equation (10) is:

$$\frac{\partial C_{as}^1}{\partial t} = k_{as} C_1^0. \quad (17)$$

Similarly, we can obtain the dimensional forms of the homogenized macroscale Equations (11) and (12) for Case 2; these have been omitted for conciseness.

Parameter values

We parameterize the model for the sandy loam soil shown in Figure 1 and a strongly-sorbed solute such as phosphate or many heavy metal and radionuclide contaminants. The soil is a Eutric Cambisol (USDA, 2014) from the experimental farm of Bangor University (properties in Lucas & Jones, 2006, Soil B). It was sieved to <1.6 mm and the solid matter of the sieved soil was approximately 0.7 g g^{-1} quartz, 0.3 g g^{-1} clay minerals (mainly illite and feldspars) and <0.03 g g^{-1} organic matter.

Geometry. We consider an experimental system where the typical length of a soil column $L = 1$ cm. We define this as the macroscale because it is the largest scale length considered in this research. In addition, we have a scale length that is associated with the soil particle size distribution. We define this as the microscale l (Figure 1). We chose $l = 0.01$ cm to cover a range of particle sizes from fine clay to coarse sand in the microscale domain. This satisfies the requirement that the scaling ratio is $\varepsilon = l/L \ll 1$, so that our two space-scale approximations are valid. We consider the effect of varying ε in 'Results and discussion' below. We obtained the value of the tensor $\mathbf{D}$ for the geometric impedance to diffusion in the soil pore space

from the X-ray CT image in Figure 1; the value is $\mathbf{D} = 0.035 \times \mathbf{I}$, where $\mathbf{I}$ is the identity matrix (Supporting Information B). For $D_l = 10^{-5}\, cm^2\, s^{-1}$, which is typical of a simple inorganic solute, the effective diffusion coefficient in the soil pore network following Equation (13) is $\mathbf{D}_{eff} = 3.5 \times 10^{-7}\, cm^2\, s^{-1}$. The mathematical procedure to obtain the effective macroscale parameters (i.e. tensor $\mathbf{E}$ and vector $\mathbf{f}$ (for slow reaction)) from the microscale domain is given in Supporting Information B. From the simulation we find the components of $\mathbf{E}_{eff}$ take a maximum value of $8.25 \times 10^{-9}\, cm^3\, s^{-1}$ and each of the components of $\mathbf{f}_{eff}$ has value $1.1 \times 10^{-7}\, cm\, s^{-1}$.

We calculated the surface area of clay minerals active in solute sorption as follows. From the X-ray CT image (Figure 1), the volume of soil solid per unit soil volume is 0.51 cm^3 cm^{-3} and the surface area of the soil solid per unit soil volume is 85.25 cm^2 cm^{-3}. Therefore, if the particle density is 2.65 g cm^{-3}, the mass of quartz, which is largely non-sorbing, per unit soil volume $= 0.7 \times 2.65 \times 0.51 = 0.95$ g cm^{-3}, and the mass of clay minerals per unit soil volume $= 0.3 \times 2.65 \times 0.51 = 0.41$ g cm^{-3}. Therefore, taking the quartz particles to be spherical with mean diameter 1.6 mm (the soil sieve size), the quartz specific surface is 14.15 cm^2 g^{-1}; therefore, the quartz surface area per unit soil volume $= 0.95 \times 14.15 = 13.43$ cm^2 cm^{-3}. The clay mineral surface area equals the total surface area minus the quartz surface area. This gives clay mineral surface area per unit volume $= 85.25 - 13.43 = 71.82$ cm^2 cm^{-3} (i.e. the clay minerals account for 84% of the total surface).

After estimating the surface area of the sorbing phase, we distributed sorption sites of equal total area over the microscale soil domain microscale soil domain. This was done by selecting portions of the soil CT-image surfaces as patches that collectively occupied 84% of the total surface (see above). We applied the sorption reactions on these spatially distributed soil surface patches following Equations (4) and (5). The remaining 16% of the total soil surface is non-sorbing; therefore, we solved Equation (3) on those surface areas. We give the mathematical detail of the distribution patterns (both uniform and non-uniform) of the sorption sites in Supporting Information A and B.

Sorption. We define the fraction of the total sorption surface area occupied by slow-reacting sites as α, such that $A_s = \alpha A_{total}$ and $A_f = (1 - \alpha) A_{total}$ where A_s and A_f are the areas of slow and fast reacting sites, respectively, per unit volume of soil, and $A_{total} = A_s + A_f$. To test the effects of varying (i) the ratio of A_s to A_f (ii) the rate of the slow sorption reaction, we derived the relations at equilibrium from Equations (4) to (5) by:

$$k_{af} C_1 - k_{df} C_{af} = 0 \quad (18)$$

and

$$k_{as} C_1 - k_{ds} C_{as} = 0. \quad (19)$$

Combining Equations (16)–(19) gives:

$$K_f = \frac{A_f k_{af}}{\theta k_{df}} \quad (20)$$

and

$$K_s = \frac{A_s k_{as}}{\theta k_{ds}}. \qquad (21)$$

We tested the effect of varying k_{as} and α (i.e. A_s/A_f) while keeping the other variables constant (see 'Results and discussion'). For the fast reaction, we used $k_{af} = 1.78 \times 10^{-5}\,\mathrm{cm\,s^{-1}}$ and $k_{df} = 2.57 \times 10^{-4}\,\mathrm{s^{-1}}$ based on the data of Keyes *et al.* (2013) for the short-term (<2 hours) kinetics of phosphate sorption on the soil in Figure 1 and $A_f = 71.82\,\mathrm{cm^2\,cm^{-3}}$ (i.e. $\theta K_f = 5$). For the slow reaction in Case 1 we used $k_{as} = 6.67 \times 10^{-7}\,\mathrm{cm\,s^{-1}}$ and $k_{ds} = 7.05 \times 10^{-8}\,\mathrm{s^{-1}}$ based on values in Ptashnyk *et al.* (2010) and $A_s = 71.82\,\mathrm{cm^2\,cm^{-3}}$ (i.e. $\theta K_s = 680$). For the slow reaction in Case 2, $k_{as} = 6.67 \times 10^{-9}\,\mathrm{cm\,s^{-1}}$ and $k_{ds} = 7.05 \times 10^{-10}\,\mathrm{s^{-1}}$.

We compare the time-scales of the fast and slow reactions with that of diffusion as follows. The half-time for diffusion into a soil column of length L maintained at a constant surface concentration is given by $\sqrt{D t_{1/2}/\pi} = L/4$ (after Crank (1979), equation 3.15). Therefore, for $D = D_l/K_f = 2 \times 10^{-6}\,\mathrm{cm^2\,s^{-1}}$ and $L = 1\,\mathrm{cm}$, the diffusion half-time is $t_{1/2} = 27.3$ hours. From the integral of Equation (4) for constant C_l, the half-time for the fast sorption reaction is $t_{1/2} = \ln 2/k_{df} = 2.7 \times 10^3\,\mathrm{s}$ or 0.75 hour, which is rapid compared with diffusion. Likewise, from Equation (5) the half-time for the slow sorption reaction is $t_{1/2} = \ln 2/k_{ds} = 9.8 \times 10^6\,\mathrm{s}$ or 114 days for Case 1, which is slow compared with diffusion. Similarly for Case 2, the half-time for the slow reaction is 1.14×10^5 days. Therefore, the representations of sorption times in the two Cases are consistent with the model assumptions.

We ran the model for a constant solute concentration in solution (representative solute concentration, C) at one end of a soil column of $10^{-4}\,\mathrm{\mu mol\,cm^{-3}}$, with zero transfer of solute across the other end of the column ($L = 1\,\mathrm{cm}$) and zero concentration initially throughout the column. The results below are for model runs of 25 days.

Model implementation

We used the open-source computational fluid dynamics software package OpenFOAM (Jasak *et al.*, 2013) for the numerical simulations with the two homogenized models, and to assess their sensitivities to the spatial distributions of sorption sites.

Results and discussion

Figure 2(a,b) shows the effects of allowing for patchy microscale distributions of sorption sites on solute concentration profiles in the soil solution and soil surface when all the sorption sites react more rapidly than rates of diffusion. It appears that microscale patchiness has little effect on macroscale transport under these conditions. If sorption is rapid compared with diffusion (i.e. half-times for equilibration <~1 hour), it is acceptable to consider the volume-averaged distribution of sorption sites without knowing their distribution patterns.

Figure 2(c,d) shows the effect of both fast and slow sorption reactions, with the slow sorption being either moderately slower (Case 1) or much slower (Case 2) than diffusion. The effect of a patchy distribution of sites is evident for Case 1, although it is only slight, but is not for Case 2. Evidently there is an interaction between the reaction rate and the patchiness effect. In Case 2, the slow reaction is so slow that it does not contribute markedly to sorption on the time-scale of the model runs; the results are therefore similar to those in Figure 2(a,b), but with a smaller degree of sorption (smaller A_f) and faster macroscale diffusion. If the slow reaction is fast enough to affect diffusion, as in Case 1, a small effect of patchiness is evident in Figure 2(c,d).

Figure 2(e,f) shows the results of when all the sorption sites react slowly. For Case 1, there is again a small effect of patchiness only. For Case 2, Figure 2(e,f) shows that there is now effectively no sorption and macroscale diffusion is correspondingly faster. Figure 3 shows the effect of a larger sorption surface area with a relatively fast slow reaction (i.e. Case 1). The concentration profiles are similar to those in Figure 2(e) (Case 1), which show no marked effect.

The results show that the effect of non-uniform distribution of sorption sites on macroscale transport is detectable only for particular combinations of reaction rate and diffusion rate, as in Case 1, and then the effect is only slight and probably too small to be detectable experimentally. Therefore, the averaging assumptions used in conventional models with equilibrium reactions are justified.

We now consider the effect of increasing the micro- to macroscale ratio, ε. For Case 1 with a slow reaction rate, a tenfold increase in ε results in a large increase in the effect of patchily distributed sorption sites (Figure 4). The distance at which C_l falls to half the value at the surface of the soil column is 0.014 cm for a uniform distribution of sites and 0.045 cm for a patchy distribution. This indicates the parameter range for which the effect of patchiness is important and correctly predicted. The effect depends on both ε and the sorption rate relative to the diffusion rate: ε must be small enough to satisfy the multiple space-scale perturbation requirements, but large enough to resolve the effect of patchiness with the right sorption rate. The reaction half-time is 114 days (Parameter values). The model suggests that for $\varepsilon = 0.1$, reaction rates 100-fold faster or slower than this will mean the reaction is either effectively instantaneous or insignificant compared with diffusion, and the effect of non-uniform distribution of sorption sites then becomes negligible. Runs with the model confirmed this (data not shown).

From a mathematical point of view, when ε is infinitely small the model predictions are exact. With an increase in ε, the error of prediction will also increase. The error is of the order $\varepsilon^2 \times 100\%$; it is just 1% for $\varepsilon = 0.1$. From a physical point of view, if we consider a soil column packed with soil particles that are small compared with the size of the column, the effect of microscale heterogeneities such as the distribution of sorption sites is insignificant. Likewise, at the pedon or field scale processes that take place on the micro-aggregate scale are irrelevant. Clearly, however, when the soil particle or aggregate size is an order of magnitude different only from the macroscale dimension that is being considered, the effects of particle or aggregate scale heterogeneities will be magnified and
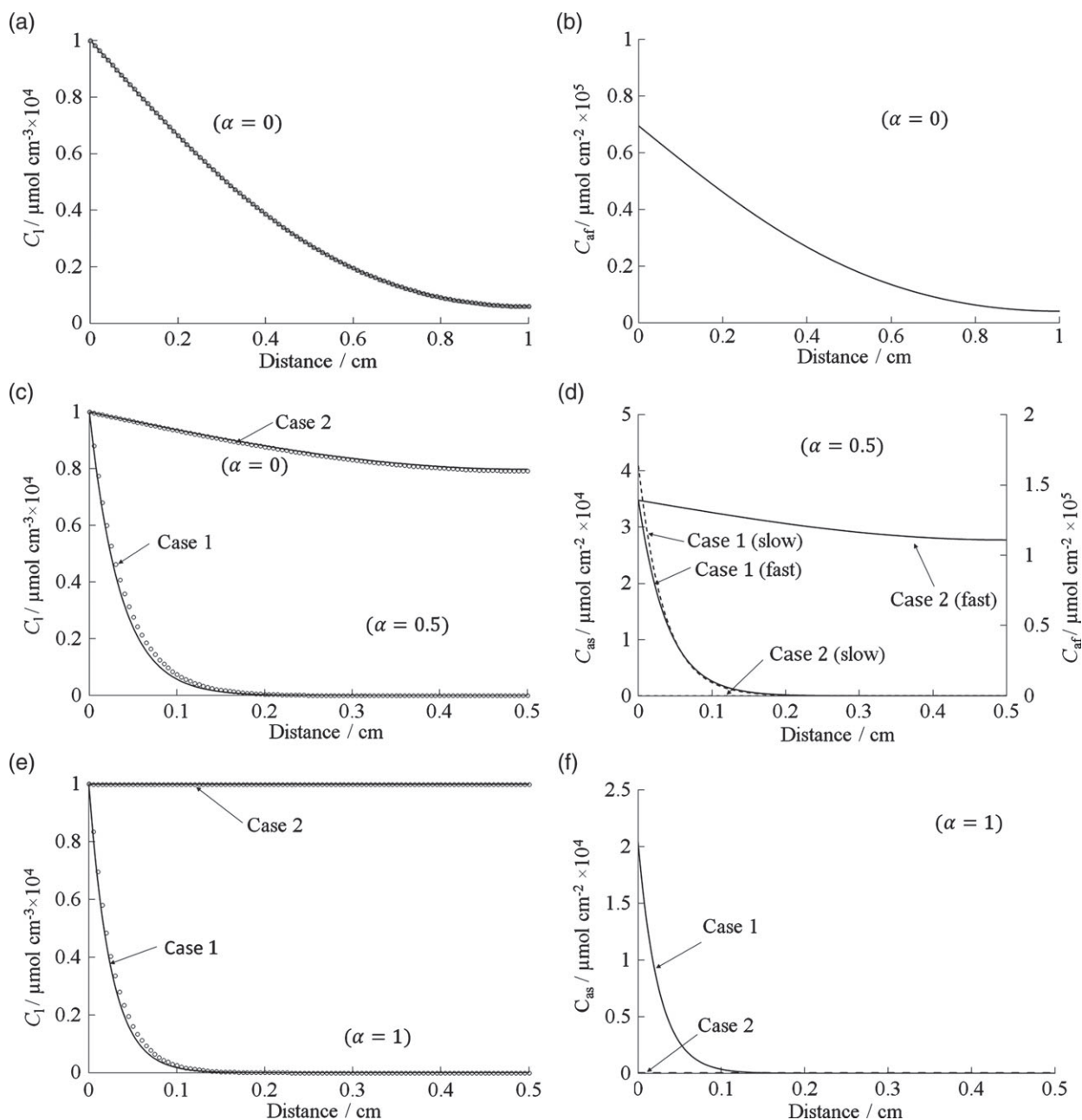
Figure 2 The effect of maintaining a constant concentration of a solute in solution at the surface of a soil column from which it was initially absent: (a, c and e) are solute concentrations in the soil solution (C_l), (b, d and f) are adsorbed solute concentrations in the soil solid (C_{af}, C_{as} for fast and slow reacting sites, respectively). (a), (b) All sorption sites were fast reacting (i.e. $\alpha = 0$). (c), (d) Half the sorption sites were fast reacting and half were slow (i.e. $\alpha = 0.5$), with slow reaction slow (Case 1) or very slow (Case 2) compared with diffusion. (e), (f) All the sorption sites were slow reacting (i.e. $\alpha = 1$) with slow reaction slow (Case 1) or very slow (Case 2) compared with diffusion. Solid lines are for a uniform distribution of sorption sites, points are for a non-uniform distribution and $t = 25$ days.

can be important. As the scaling ratio, ε, increases, the microscopic grain becomes closer to macroscopic soil and therefore imposes an increasing effect on model predictions.

The above conclusions are consistent with equivalent research on solute transport in groundwater systems (Bellin *et al.*, 1993; Bosma *et al.*, 1993; Espinoza & Valocchi, 1997; Dentz *et al.*, 2011). Meile

& Tuncay (2006) showed, based on pore-scale simulations, that in diffusion-driven transport the effect of non-homogeneity in reaction rates has only a small effect on the macroscale reactions.

The above conclusions will not necessarily hold if the solute reaction rates or other sources or sinks of the solutes themselves depend on microscale heterogeneities. The microscale distribution of
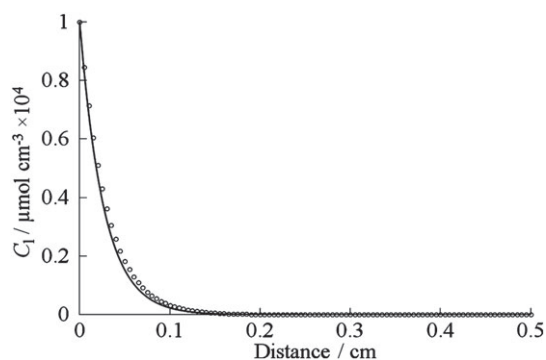
Figure 3 Concentration-distance profiles in the soil solution as in Figure 2 for a tenfold larger sorption surface area (i.e. $1.1 \times A_{total}$). All sorption sites were slow reacting (i.e. $\alpha = 1$), with reaction rates fast enough to affect diffusion (i.e. Case 1). Solid lines are for a uniform distribution of sorption sites, points are for a non-uniform distribution and $t = 25$ days.
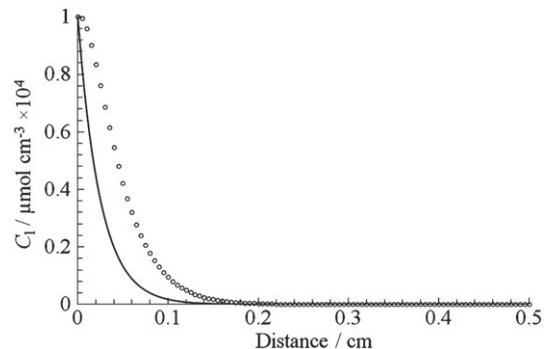

Figure 4 Concentration-distance profiles in the soil solution as in Figure 2 for micro- to macroscale ratio $(\varepsilon) = 0.1$ (i.e. tenfold smaller than in Figure 2). All sorption sites were slow reacting (i.e. $\alpha = 1$), with reaction rates fast enough to affect diffusion (i.e. Case 1). Solid lines are for a uniform distribution of sorption sites, points are for a non-uniform distribution and $t = 25$ days.

sorption sites might then be important. An example is the uptake of solutes by root hairs, which have lengths comparable to the soil geometric microscale (Keyes *et al.*, 2013). Soil processes at such scales are increasingly measurable with non-invasive imaging techniques. Another example is the microbially-mediated turnover of soil organic matter, which Falconer *et al.* (2015) show, with a model that allows for non-linear microbial growth kinetics, depends strongly on the microscale distribution of both nutrients and microbes and associated local transport limitations. This implies that macroscale models of soil carbon turnover should account for microscale heterogeneities explicitly. This could be achieved with our modelling approach by incorporating the microbial growth kinetics in the microscale equations (the equivalents to Equations 2 and 3).

For simplicity, we considered a water-saturated soil in our simulations. Our approach could be applied easily to non-saturated soil, however. The geometry we have used is taken from X-ray CT images in which air and water can be clearly distinguished. By treating the air–water interface within a pore as a non-sorbing site,

we could model partially saturated soil in the same way as saturated soil. The same macroscopic equations will apply, but the model parameters derived from the pore geometry will be different.

We have not considered advection. In general, for strongly-sorbed solutes rates of advection are small and diffusion is the dominant transport process (Roose & Kirk, 2009). Our approach could also be used, however, for cases where advection is important, such as for weakly sorbed solutes.

Conclusions

We have found that, in general, the distribution of sorption sites at the microscale has little effect on diffusion at the macroscale. This indicates that, in most cases, the assumption implicit in most conventional solute transport models that microscale heterogeneities are unimportant at the macroscale, is justified. Microscale heterogeneities, however, do become important if (i) the ratio of the micro- to macro-length scales, ε, is large and (ii) solute sorption on soil surfaces is slow relative to diffusion, but not so slow that it does not affect diffusion. Nevertheless, if we consider a small sample of soil, such as is often used in synchrotron computed-tomography experiments, then the effect of microscale heterogeneities at sorption sites will be significant. The modelling error will also be amplified, varying as $100 \times \varepsilon^2\%$. It will, however, remain smaller than the effects of the distribution of sorption sites.

Supporting Information

The following supporting information is available in the online version of this article:
Supplementary Information, SI: Further modelling details.

Acknowledgements

References

Bellin, A., Rinaldo, A., Bosma, W.J.P., Zee, S.E. & Rubin, Y. 1993. Linear equilibrium adsorbing solute transport in physically and chemically heterogeneous porous formations: 1. Analytical solutions. *Water Resources Research*, **29**, 4019–4030.

Blunt, M.J., Bijeljic, B., Dong, H., Gharbi, O., Iglauer, S., Mostaghimi, P. *et al.* 2013. Pore-scale imaging and modelling. *Advances in Water Resources*, **51**, 197–216.

Bosma, W.J.P., Bellin, A., Van der Zee, S. & Rinaldo, A. 1993. Linear equilibrium adsorbing solute transport in physically and chemically heterogeneous porous formations: 2. Numerical results. *Water Resources Research*, **29**, 4031–4043.

Burridge, R. & Keller, J.B. 1981. Poroelasticity equations derived from microstructure. *The Journal of the Acoustical Society of America*, **70**, 1140–1146.

Crank, J. 1979. *The Mathematics of Diffusion*. Oxford University Press, Oxford.

Daly, K.R., Mooney, S., Bennett, M., Crout, N., Roose, T. & Tracy, S. 2015. Assessing the influence of the rhizosphere on soil hydraulic properties using X-ray Computed Tomography and numerical modelling. *Journal of Experimental Botany*, **66**, 2305–2314.

Dentz, M., Le Borgne, T., Englert, A. & Bijeljic, B. 2011. Mixing, spreading and reaction in heterogeneous media: a brief review. *Journal of Contaminant Hydrology*, **120**, 1–17.

Espinoza, C. & Valocchi, A.J. 1997. Stochastic analysis of one-dimensional transport of kinetically adsorbing solutes in chemically heterogeneous aquifers. *Water Resources Research*, **33**, 2429–2445.

Falconer, R.E., Battaia, G., Schmidt, S., Baveye, P., Chenu, C. & Otten, W. 2015. Microscale heterogeneity explains experimental variability and non-linearity in soil organic matter mineralisation. *PLoS One*, **10**, e0123774. doi: 10.1371/journal. pone.0123774.

Hornung, U. 1997. *Homogenization and Porous Media*. Springer-Verlag, Berlin.

Jasak, H., Jemcov, A. & Tukovic, Z. 2013. *OpenFOAM: A C++ Library for Complex Physics Simulations.*

Keller, J.B. 1980. Darcy's law for flow in porous media and the two-space method. In: *Nonlinear Partial Differential Equations in Engineering and Applied Science* (ed. R.L. Sternberg), pp. 429–443. Dekker, New York.

Keyes, S.D., Daly, K.R., Gostling, N.J., Jones, D.L., Talboys, P., Pinzer, B.R. *et al.* 2013. High resolution synchrotron imaging of wheat root hairs growing in soil and image based modelling of phosphate uptake. *New Phytologist*, **198**, 1023–1029.

Lee, C.K. & Mei, C.C. 1997. Re-examination of the equations of poroelasticity. *International Journal of Engineering Science*, **35**, 329–352.

Leitner, D., Schnepf, A., Klepsch, S. & Roose, T. 2010. Comparison of nutrient uptake between three-dimensional simulation and an averaged root system model. *Plant Biosystems*, **144**, 443–447.

Lucas, S.D. & Jones, D.L. 2006. Biodegradation of estrone and 17 beta-estradiol in grassland soils amended with animal wastes. *Soil Biology & Biochemistry*, **38**, 2803–2815.

Meile, C. & Tuncay, K. 2006. Scale dependence of reaction rates in porous media. *Advances in Water Resources*, **29**, 62–71.

Pavliotis, G. & Stuart, A. 2008. *Multiscale Methods: Averaging and Homogenization*. Springer Science & Business Media, Berlin.

Ptashnyk, M., Roose, T. & Kirk, G.J.D. 2010. Diffusion of strongly sorbed solutes in soil: a dual-porosity model allowing for slow access to sorption sites and time-dependent sorption reactions. *European Journal of Soil Science*, **61**, 108–119.

Roose, T. & Kirk, G.J.D. 2009. The solution of convection–diffusion equations for solute transport to plant roots. *Plant and Soil*, **316**, 257–264.

Tinker, P.B. & Nye, P.H. 2000. *Solute Movement in the Rhizosphere*, 2nd edn. Oxford University Press, New York.

Tracy, S.R., Daly, K.R., Sturrock, C.J., Crout, N.M.J., Mooney, S.J. & Roose, T. 2015. Three dimensional quantification of soil hydraulic properties using X-ray Computed Tomography and image based modelling. *Water Resources Research*, **51**, 1006–1022.

USDA 2014. *Keys to Soil Taxonomy*. Natural Resources Conservation Service, Washington.

Wildenschild, D. & Sheppard, A.P. 2013. X-ray imaging and analysis techniques for quantifying pore-scale structure and processes in subsurface porous medium systems. *Advances in Water Resources*, **51**, 217–246.

Zygalakis, K.C., Kirk, G.J.D., Jones, D.L., Wissuwa, M. & Roose, T. 2011. A dual porosity model of nutrient uptake by root hairs. *New Phytologist*, **192**, 676–688.